

## Logic Gates and Elementary Computing by Enzymes<sup>†</sup>

Ronan Baron, Oleg Lioubashevski, Eugenio Katz, Tamara Niazov, and Itamar Willner\*

*Institute of Chemistry, The Hebrew University of Jerusalem, Jerusalem 91904, Israel*

*Received: November 24, 2005; In Final Form: February 7, 2006*

Different selected enzymes, glucose oxidase (GOx), catalase (Cat), glucose dehydrogenase (GDH), horseradish peroxidase (HRP), and formaldehyde dehydrogenase (FDH), are used alone or coupled to construct eight different logic gates. The added substrates for the respective enzymes, glucose and H<sub>2</sub>O<sub>2</sub>, act as the gate inputs, while the biocatalytically generated gluconic acid or NADH are the output signals that follow the operation of the gates. Different enzyme-based gates are XOR, INHIBIT A, INHIBIT B, AND, OR, NOR, Identity and Inverter gates. By combining the AND and XOR or the XOR and INHIBIT A gates, the half-adder and half-subtractor are constructed, respectively, opening the way to elementary computing by the use of enzymes.

### Introduction

During the last few years, tremendous efforts have been directed toward the construction of molecule- or biomolecule-based logic gates and computing elements. Extensive research efforts were directed in recent years toward the application of molecules or supramolecular structures to mimic the functions of logic gates.<sup>1–4</sup> For example, de Silva et al. demonstrated a molecular AND gate that consisted of a pH-sensitive chromophore and a receptor site.<sup>5</sup> The protonated receptor, lacking fluorescence, was bound to the receptor site. Deprotonation of the chromophore and binding of Ca<sup>2+</sup> to the receptor acted as two stimuli that activated the fluorescence of the chromophore, and led to an AND gate. Similarly, an OR logic gate was exemplified with the synthesis of a multifunctional structure consisting of two anthracene units tethered by oligoethylene glycol to a 2,2'-bipyridine site.<sup>6</sup> The binding of Na<sup>+</sup> to the oligoethylene glycol chains (stimuli 1) or the association of Hg<sup>2+</sup> (stimuli 2) to the bipyridine unit resulted in a sterically favored configuration of anthracene units for photodimerization. The quantum yield for photodimerization of anthracene was then used as the OR gate readout signal. Also, photoisomerization of a phenoxynaphthalene quinone monolayer associated with an electrode, and coupled to the electrocatalytic reduction of a bipyridinium electron acceptor unit, was reported to act as a surface integrated AND gate.<sup>1e,7</sup> Light signals and pH were employed as triggering stimuli for the reduction of the bipyridinium electron acceptor, and the resulting amperometric response from the system was employed as a transduction signal for the AND gate operation. The parallel operation of logic gates enabled the use of molecular assemblies for arithmetic operations.<sup>4</sup> For example, molecular structures that perform the binary addition were developed. A half-adder system was demonstrated through the combination of XOR and AND logic gates, whose outputs code the sum and carry digits. Recently, the operation of a simple molecule as half-adder or half-subtractor was demonstrated.<sup>3c</sup> The need for acid/base stimuli to activate these functions represents, however, a drawback due to the volume change of the system associated with the application of the

triggering signals. The use of biomaterials as active computing elements also attracts substantial research effort.<sup>8,9</sup> For example, gene-based artificial circuits analogous to a bistable toggle switch<sup>9a</sup> or to an oscillator<sup>9b</sup> were designed. DNA and enzymes were also coupled to perform programmable biochemical transformations that mimic basic computing of finite automaton,<sup>9c</sup> leading to a biological computer that logically analyzes the content of RNA and produces as an output a molecule that controls the levels of gene expression.<sup>9e</sup> However, although theoretically addressed more than 40 years ago by Sugita<sup>10</sup> and more recently by Arkin and Ross,<sup>11</sup> very few studies dealt with the use of enzymes as building blocks for computing architectures. A XOR gate was constructed using the conformational dynamics of malate dehydrogenase in response to the addition of Mg<sup>2+</sup> and Ca<sup>2+</sup>, and the possibility of making other gates was discussed.<sup>12</sup> Moreover, an AND gate was obtained using a modified enzyme and its inhibitor.<sup>13</sup> In the present study, we demonstrate that a large variety of logic gates that share common inputs can be designed using single or coupled native enzymes. By applying a simple spectrophotometric method, the outputs originating from the logic gate functions are read out. Furthermore, we demonstrate that by using several of the designed gates, binary addition and subtraction operations were carried out.

### Experimental Procedures

**Materials and Methods.** All enzymes and chemicals were purchased from Aldrich or Sigma. The enzymes that were used are glucose dehydrogenase from *Thermoplasma acidophilum* (E.C. 1.1.1.47), peroxidase from horseradish (E.C. 1.11.1.7), glucose oxidase from *Aspergillus niger* (E.C. 1.1.3.4), catalase from bovine liver (E.C. 1.11.1.6), and formaldehyde dehydrogenase from *Pseudomonas putida* (E.C. 1.2.1.46). The absorbance measurements were performed using a Shimadzu UV-2401PC UV–vis spectrophotometer. All measurements were done at 25 ± 2 °C.

**Experimental Conditions.** The inputs that were used for all the gates corresponded to an addition of 0.30 M H<sub>2</sub>O<sub>2</sub> (input A) and 1 M β-D(+)-glucose (input B). The output for all the gates corresponds to the variations in the absorbance, |ΔA|, measured after a time interval of 20 min. The absorbance

<sup>†</sup> Part of the "Chava Lifshitz Memorial Issue".

\* Corresponding author. Tel.: 972-2-6585272; fax: 972-2-6527715; e-mail: willnea@vms.huji.ac.il.

variation is the absolute value of the difference of absorbance before and after the enzymatic reaction takes place. For the XOR, INHIBIT A, INHIBIT B, OR, NOR, and Inverter gates,  $|\Delta A|$  was measured at 340 nm and corresponded to the variation of the amount of NADH in the medium. For the AND and Identity gates,  $|\Delta A|$  was measured at 500 nm and corresponded to the variation of the amount of gluconic acid in the media. Gluconic acid was detected in the different systems spectrophotometrically at 500 nm after its reaction with hydroxylamine and subsequent complexation of the generated hydroxamate with Fe(III).<sup>14</sup> The measurements were done in a 500  $\mu\text{L}$  spectrophotometric quartz cell, allowing measurements in a volume as little as 250  $\mu\text{L}$ .

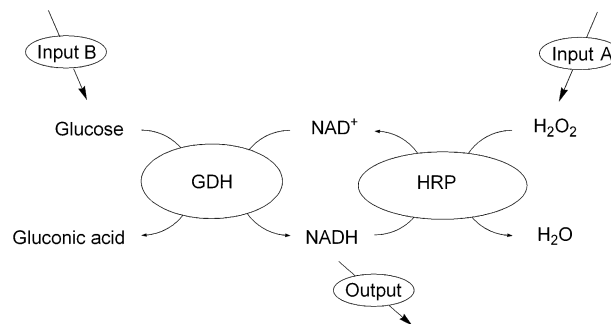
**Composition of the Gates.** The XOR gate system consisted of a 250  $\mu\text{L}$  solution of horseradish peroxidase, 10 U; glucose dehydrogenase, 7.5 U;  $\text{NAD}^+$ ,  $1 \times 10^{-4}$  M; and NADH,  $1 \times 10^{-4}$  M, in 0.01 M phosphate buffer, pH = 6.8 (the amounts of enzymes were balanced in such a way that the biocatalytic transformations proceeded at the same rates). The INHIBIT B gate system was composed of a 250  $\mu\text{L}$  solution of horseradish peroxidase, 2.5 U; glucose dehydrogenase, 7.5 U; and NADH,  $1 \times 10^{-4}$  M, in 0.05 M phosphate buffer, pH = 6. The INHIBIT A gate system consisted of a 250  $\mu\text{L}$  solution of horseradish peroxidase, 13.5 U; glucose dehydrogenase, 3 U; and  $\text{NAD}^+$ ,  $1 \times 10^{-4}$  M, in 0.01 M phosphate buffer, pH = 6.8. The AND gate system was composed of a 500  $\mu\text{L}$  solution of glucose oxidase, 20 U; catalase, 200 U; and 0.01 M phosphate buffer, pH = 7.3. For this later system, the reaction medium was degassed with argon that was purified from oxygen traces by bubbling through a sodium dithionite/methyl viologen aqueous solution. The OR gate system was composed of a 250  $\mu\text{L}$  solution of horseradish peroxidase, 30 U; glucose oxidase, 170 U; and NADH,  $1 \times 10^{-4}$  M, in 0.05 M phosphate buffer, pH = 6. The NOR gate system was composed of a 250  $\mu\text{L}$  solution of formaldehyde dehydrogenase, 0.15 U; glucose oxidase, 500 U;  $\text{NAD}^+$ ,  $2 \times 10^{-4}$  M; and formaldehyde,  $1 \times 10^{-4}$  M, in 0.01 M phosphate buffer, pH = 7.3. The Identity gate system was composed of a 250  $\mu\text{L}$  solution of glucose oxidase, 20 U, in a 0.01 M phosphate buffer, pH = 7.3. The Inverter gate was composed of a 250  $\mu\text{L}$  solution of formaldehyde dehydrogenase, 0.15 U, and formaldehyde,  $1 \times 10^{-4}$  M, in a 0.01 M phosphate buffer, pH = 7.3.

## Results and Discussion

The two chemical inputs were hydrogen peroxide (input A) and glucose (input B); they were used at equal concentrations for all gates. The output of the biocatalytic logic gates (the result of the enzymatic activity of the systems) was read out in terms of the absorbance change at appropriate wavelengths. For each of the designed gates, two regions for the absorbance changes,  $|\Delta A|$ , were defined. One region of the absorbance change,  $|\Delta A|$ , from 0 to 0.08 was defined as the low level output and corresponded to a logical 0, and an absorbance change ranging from 0.2 to 1.2 was defined as a high level output, and it corresponded to a logical 1 (for the definition of the low and high value of the absorbance changes corresponding to the NOR and INHIBIT B vide infra). It should be noted that the presentation of the absorbance changes in the form of a modulus can be implemented by available electronic circuits that could be integrated into the analyzing spectrophotometer. Also, for all systems, a TRUE input was marked as input configuration 1, whereas a FALSE input was presented as an input configuration 0.

The XOR gate was obtained using glucose dehydrogenase, GDH; horseradish peroxidase, HRP; and equal amounts of

## SCHEME 1: Representation of the XOR, INHIBIT A, and INHIBIT B Biocatalytic Gates



NADH and  $\text{NAD}^+$  (Scheme 1). The output was the absolute value of the variation of absorbance,  $|\Delta A|$ , of the NADH absorbance change measured at  $\lambda = 340$  nm, after the enzymatic reaction took place for a time interval of 20 min. The selection of the time interval of 20 min originated from the fact that the absorbance values of the systems were close to the saturation values. Figure 1A shows a high absorbance variation at 340 nm (output 1) only for the configurations of inputs (1,0) and (0,1). When only glucose was added to the system, (input B in configuration 1 and input A in configuration 0), then the GDH reduced  $\text{NAD}^+$  to NADH, leading to a variation of absorbance changes of NADH (curve c), while if only  $\text{H}_2\text{O}_2$  was added (input A in configuration 1 and input B in configuration 0), then the HRP biocatalyzed oxidation of NADH to  $\text{NAD}^+$  proceeded, resulting in a negative change in the absorbance of NADH (curve b). When inputs were in the configuration (1,1), the introduced glucose created NADH, and the addition of  $\text{H}_2\text{O}_2$  consumed NADH. The result of both processes was a low absorbance change at 340 nm (curve d). The absorbance variations of the XOR gate operation and the corresponding truth table are presented in Figure 1B,C, respectively.

The INHIBIT A (or InhibAND) gate was obtained, as in the case of the XOR gate, using GDH and HRP (Scheme 1). The INHIBIT A gate had an output 1 only if input A was in configuration 0, while input B was in configuration 1. A combination of two inputs in configuration 1 gave an output 0. This INHIBIT A (or InhibAND) gate required the addition of  $\text{NAD}^+$  in the medium in the absence of NADH. The absorbance of NADH was followed spectrophotometrically. If both inputs were FALSE, configuration (0,0), there was no NADH produced, as shown in Figure 1D, curve a. Addition of  $\text{H}_2\text{O}_2$  alone, configuration (1,0), also did not lead to the production of NADH (curve b). Addition of glucose alone, configuration (0,1), allowed the GDH-mediated reduction of  $\text{NAD}^+$  to NADH and gave an output 1, curve c. When inputs were in configuration (1,1), the GDH catalytically reduced  $\text{NAD}^+$  to NADH, but the HRP-mediated oxidation of NADH by  $\text{H}_2\text{O}_2$  regenerated  $\text{NAD}^+$ . The result of these two processes was that no variation in absorbance took place at  $\lambda = 340$  nm, curve d. The absorbance variations and the truth table of the INHIBIT A gate are presented in Figure 1E,F, respectively. The observation of an absorbance peak at  $\lambda = 410$  nm corresponds to the reduced heme site of HRP.

The INHIBIT B gate is basically the equivalent of the INHIBIT A gate, except for the fact that the output 1 was obtained for input A in configuration 1. The INHIBIT B gate was also obtained using GDH and HRP (Scheme 1). To obtain this gate, NADH was introduced in the system in the absence of  $\text{NAD}^+$ . The output corresponds to the variation of the absorbance of NADH followed spectroscopically at  $\lambda = 340$  nm. The low level and high level absorbance changes for the INHIBIT B gate were defined as 0–0.09, logical 0, and 0.12–

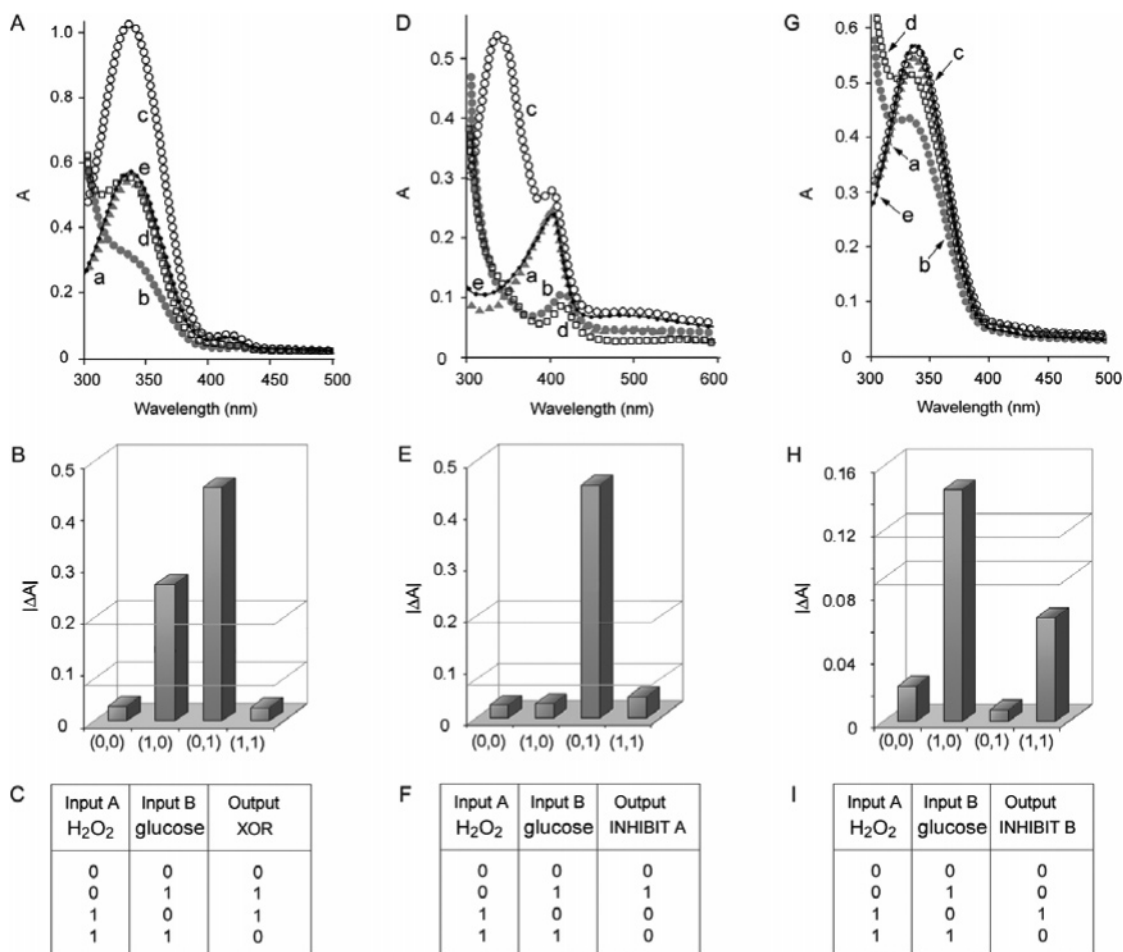


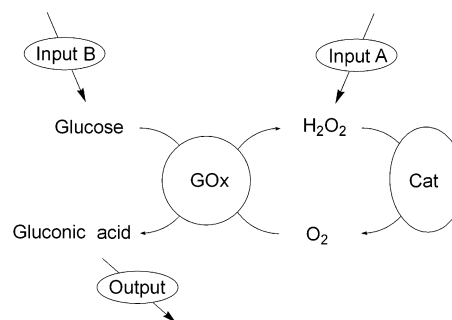
**Figure 1.** (A) Absorbance features of the XOR gate. (B) Bar presentation of the XOR gate absorbance outputs at  $\lambda = 340$  nm. (C) Truth table corresponding to the XOR gate. (D) Absorbance features of the INHIBIT A gate. (E) Bar presentation of the INHIBIT A gate absorbance outputs at  $\lambda = 340$  nm. (F) Truth table for the INHIBIT A gate. (G) Absorbance features of the INHIBIT B gate. (H) Bar presentation of the INHIBIT B gate absorbance outputs at  $\lambda = 340$  nm. (I) Truth table for the INHIBIT B gate. For all spectra, inputs correspond to (a) 0,0; (b) 1,0; (c) 0,1; (d) 1,1; and curve (e) corresponds to the absorbance of the biocatalytic system prior to activation by the inputs. For all bar presentations, absorbance variation values are marked by surfaces separating the regions of output 0 from the output 1. For all systems, GDH and HRP coupled by the NAD<sup>+</sup>/NADH cofactor system are used as the biocatalytic processors.

0.2, logical 1, respectively. In this configuration, a significant consumption of NADH by HRP can be obtained only when H<sub>2</sub>O<sub>2</sub> is introduced in the system. But if the inputs are in the configuration (1,1), the amounts of the enzymes are equilibrated in such a way that the amount of NADH that is consumed by HRP is immediately compensated by the amount produced by GDH. Then, a significant variation of the absorbance of NADH is obtained only for the situation (1,0), that is, when input B is in configuration 0 and input A is in configuration 1, Figure 1G, curve b. The bar presentation for the output is given Figure 1H, and the truth table is presented Figure 1I.

For the AND gate, the system was composed of the two enzymes Cat and GOx working under an inert Ar atmosphere in a hermetically sealed vial, Scheme 2. The catalase-mediated transformation of input A yielded O<sub>2</sub> that was consumed by GOx catalyzing the oxidation of input B, glucose, to gluconic acid. The gluconic acid product corresponded to the output, and it was colorimetrically analyzed. From the spectra depicted in Figure 2A, it can be seen that the product is generated (output 1) only if both inputs are present in the system, curve d. This is also shown by the absorbance changes presented in Figure 2B. This situation corresponds to the AND gate as shown in the respective truth table, Figure 2C.

For the OR gate, the system is composed of the two enzymes GOx and HRP and the cofactor NADH, Scheme 3. The output

#### SCHEME 2: Representation of the Biocatalytic AND Gate



signal is the modulus,  $|\Delta A|$ , of the NADH absorbance change at  $\lambda = 340$  nm, measured after the reaction was allowed to proceed for 20 min. Upon the introduction of glucose in the system (input B in configuration 1), GOx yielded H<sub>2</sub>O<sub>2</sub> that was then consumed by the HRP catalyzing the oxidation of NADH to NAD<sup>+</sup>, resulting in the depletion of NADH and an absorbance change. If H<sub>2</sub>O<sub>2</sub> was added to the system (input A in configuration 1), or both input A and input B were introduced, the same oxidation of NADH to NAD<sup>+</sup> proceeded. This is, indeed, verified experimentally, and NAD<sup>+</sup> is generated, Figure 2D, curves b–d. The absorbance changes are presented in Figure

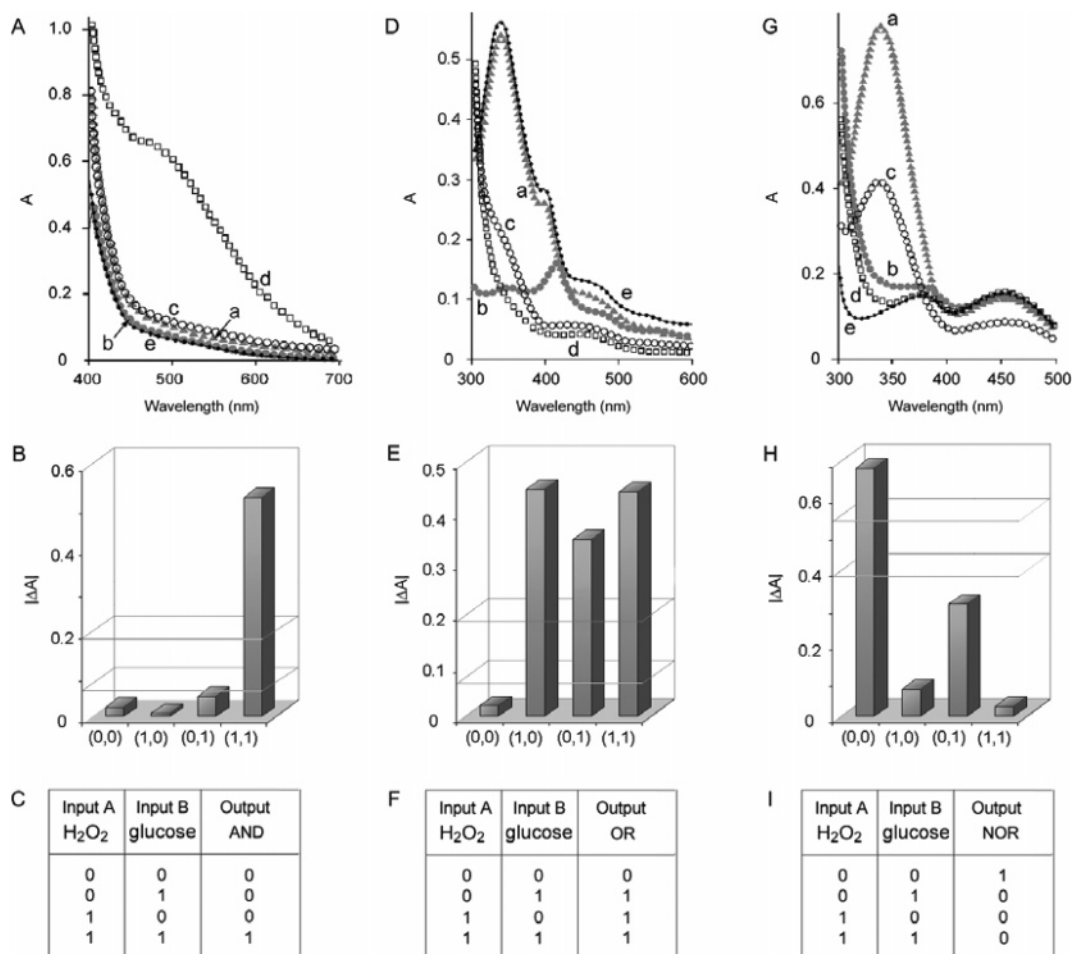
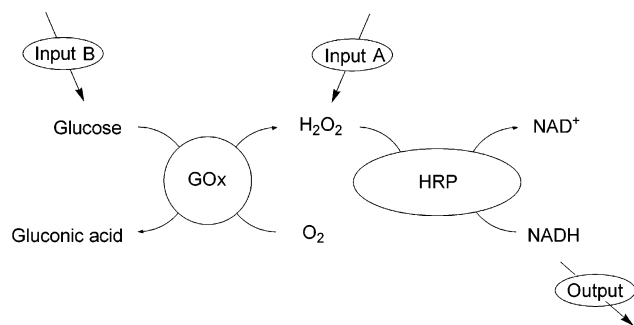


**Figure 2.** (A) Absorbance features of the AND gate. (B) Bar presentation of the AND gate absorbance outputs at  $\lambda = 500$  nm. (C) Truth table corresponding to the AND gate. (D) Absorbance features of the OR gate. (E) Bar presentation of the absorbance outputs of the OR gate at  $\lambda = 340$  nm. (F) Truth table for the biocatalytic OR gate. (G) Absorbance features of the NOR gate. (H) Bar presentation of the absorbance outputs corresponding to the NOR gate at  $\lambda = 340$  nm. (I) Truth table for the NOR gate. For all spectra, inputs correspond to (a) 0,0; (b) 1,0; (c) 0,1; and (d) 1,1, and curve e corresponds to the absorbance of the biocatalytic system prior to activation by the inputs. For all bar presentations, absorbance variation values are marked by surfaces separating the regions of output 0 from the output 1. For the AND gate, GOx and Cat are used as the biocatalytic processors. For the OR gate, GOx and HRP are used as the biocatalytic processors. For the NOR gate, GOx and FDH are used as the biocatalytic processors.

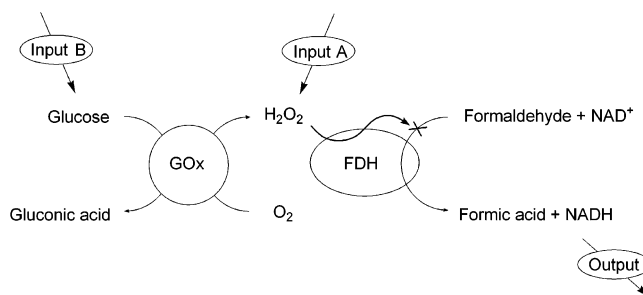
### SCHEME 3: Representation of the Biocatalytic OR Gate



2E, and the respective truth table corresponding to the OR gate is given in Figure 2F.

To tailor the NOR gate, the system was composed of coupled enzymes GOx and FDH, Scheme 4. Formaldehyde and NAD<sup>+</sup> are also added to the system just before starting the experiment, and the product is the generated NADH that is followed by the absorbance change at  $\lambda = 340$  nm. The low level and high level absorbance changes for the NOR gate are defined as 0–0.4, logical 0, and 0.55–0.8, logical 1, respectively. It is known from the literature that H<sub>2</sub>O<sub>2</sub> is a strong inhibitor for the biocatalytic

### SCHEME 4: Representation of the Biocatalytic NOR Gate



oxidation of formaldehyde by FDH from *P. putida*.<sup>15</sup> This inhibition by H<sub>2</sub>O<sub>2</sub> implies that, when H<sub>2</sub>O<sub>2</sub> is introduced or produced in the system, the reduction of NAD<sup>+</sup> is inhibited, thus giving an output signal 0. From the spectra depicted in Figure 2G, it can be seen, as expected, that NADH is generated only if inputs are in configuration (0,0), curve a. The absorbance changes presented in Figure 2H show that an output of 1 exists only for a situation when the inputs are (0,0) in agreement with the respective truth table, Figure 2I.

Two other gates that were developed require only the use of a single enzyme system: the Identity and Inverter gates. The

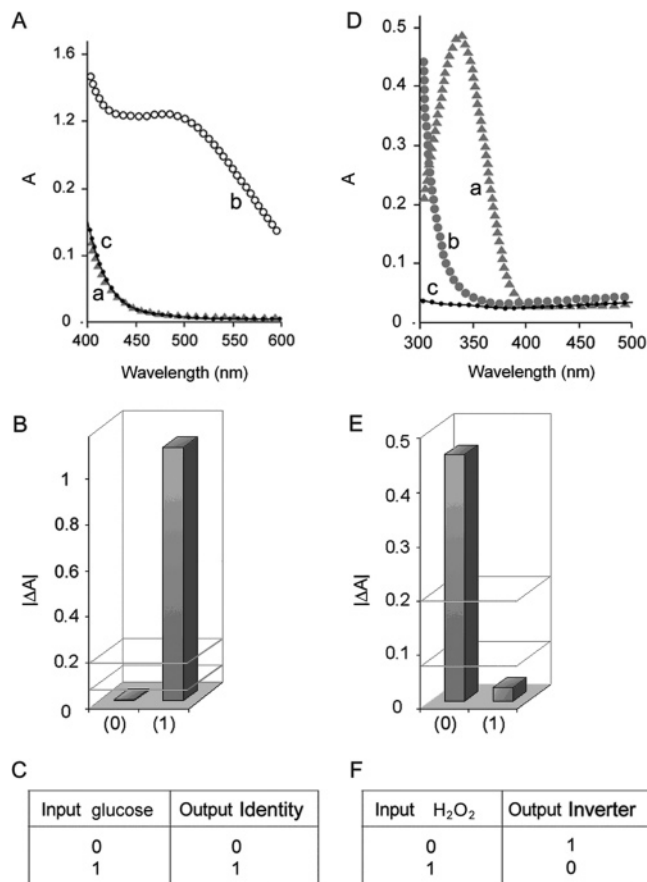
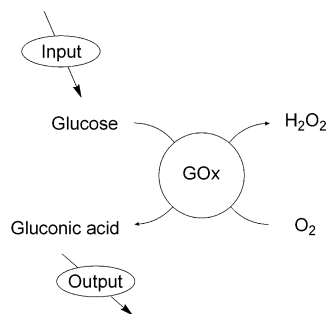


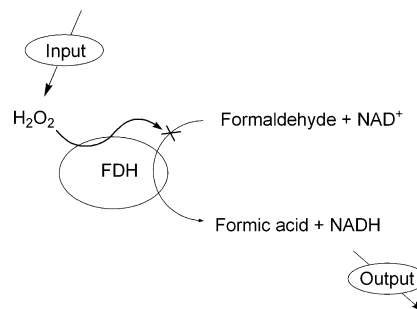
**Figure 3.** (A) Absorbance features of the Identity gate. (B) Bar presentation of the Identity gate absorbance outputs at  $\lambda = 500$  nm. (C) Truth table corresponding to the Identity gate. (D) Absorbance features of the Inverter gate. (E) Bar presentation of the Inverter gate absorbance outputs at  $\lambda = 340$  nm. (F) Truth table corresponding to the Inverter gate. For the spectra, inputs correspond to (a) 0 and (b) 1, and curve c corresponds to the absorbance of the biocatalytic system prior to activation by the inputs. For all bar presentations, absorbance variation values are marked by surfaces separating the regions of output 0 from the output 1. For the Identity gate, GOx is used as the biocatalytic processor. For the NOT gate, FDH is used as the biocatalytic processor.

#### SCHEME 5: Representation of the Biocatalytic Identity Gate



Identity and Inverter gates are elementary gates that require only one input, glucose, for the Identity gate and  $H_2O_2$  for the Inverter gate. For these gates, the introduction of the other input to the system will have no effect. For the Identity gate, the system was composed of GOx in a phosphate buffer solution, Scheme 5. Similarly, to the AND gate, the variation of absorbance due to the production of gluconic acid was the output. Basically, if the input is in configuration 1, and only if it is in this configuration, glucose is transformed to gluconic acid by GOx,

#### SCHEME 6: Representation of the Biocatalytic NOT Gate



#### SCHEME 7: Schematic Representation of the Half-Adder (HA) and Half-Subtractor (HS)

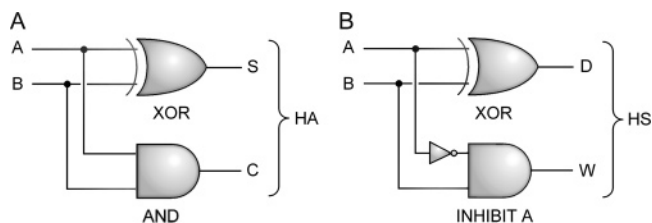


**TABLE 1: Truth Table for the Half-Adder**

input A	input B	AND gate output, carry digit	XOR gate output, sum digit	binary sum
0	0	0	0	00
0	1	0	1	01
1	0	0	1	01
1	1	1	0	10

**TABLE 2: Truth Table for the Half-Subtractor**

input A	input B	INHIBIT A gate output, borrow digit	XOR gate output, difference digit	binary subtraction
0	0	0	0	00
0	1	1	1	11
1	0	0	1	01
1	1	0	0	00

and it gives an output 1. The experimental absorbance curves are shown in Figure 3A, and the variation of absorbance is detailed in Figure 3B. The truth table for the Identity gate is given in Figure 3C.

As far as the Inverter (or NOT) gate is concerned, we selected FDH from *P. putida* as an enzyme. This biocatalyst was also employed in the NOR gate, and as mentioned, it is inhibited by  $H_2O_2$ .<sup>15</sup> Scheme 6. The variation of absorbance of NADH is the output signal. When the input was in configuration 0 (absence of  $H_2O_2$ ), FDH catalyzed both the oxidation of formaldehyde to formic acid and the reduction of  $NAD^+$  to NADH. On the contrary, when  $H_2O_2$  was introduced to the system (input in configuration 1), the enzymatic activity was inhibited, and thus no (or very low) change in the absorbance at 340 nm occurred, leading to an output 0. The spectra and the respective absorbance change at 340 nm are presented in Figure 3D,E, respectively. The results indicate that the biocatalytic Inverter gate is, indeed, experimentally materialized. The truth table for the Inverter gate is presented in Figure 3F.

The variety of logic gates that were developed allowed us to combine the operation of the gates and eventually to run them in parallel to perform algebraic operations. The half-adder is obtained by combining the AND and XOR gates, Scheme 7A.

The truth table for the half-adder is given in Table 1. The output of the AND gate is the carry digit (C), and the output of the XOR gate is the sum digit (S). The parallel operation of the two enzyme-based gates is capable of carrying out the binary operations  $0 + 0 = 0$ ;  $0 + 1 = 1$ ;  $1 + 0 = 1$ ; and  $1 + 1 = 10$ . Similarly, a half-subtractor, performing  $a - b$  algebraic operations, is obtained using both the INHIBIT A and the XOR gates, Scheme 7B. The truth table for the half-subtractor is given in Table 2. The output of the INHIBIT A gate is the borrow digit (W), and the output of the XOR gate is the difference digit (D). Thus, the system performs the following binary subtractions:  $0 - 0 = 0$ ;  $0 - 1 = 11$  (which corresponds to  $-1$ , according to conventional notations in computer science<sup>16</sup>);  $1 - 0 = 1$ ; and  $1 - 1 = 0$ . Thus, the use of coupled enzymes operating in parallel allows the execution of simple arithmetic operations: addition and subtraction.

It should be noted that throughout the paper, we defined absorbance cutoff regions as indicators for 1 or 0 outputs. The definition of regions is analogous to the electronic computers, where the 0/1 outputs are defined by voltage regions. Although in the present study the threshold absorbance values were different for the various gates, one should note that upon optimization of the concentrations of the inputs, one may define common cutoff regions.

## Conclusions

Our study has demonstrated that coupled enzyme systems and their respective substrates may be used as ingredients for the construction of a variety of logic gate operations. We have constructed the XOR, INHIBIT A, INHIBIT B, AND, OR, and NOR gates and the elementary Identity and Inverter gates. Moreover, we have shown that by the parallel operation of the AND and XOR gates, or of the INHIBIT A and XOR gates, half-adder and half-subtractor systems were constructed. Although the fundamental goal of the present study was to demonstrate a proof-of-concept, where biocatalytic transformations enable the performance of logic operations, such as the addition or subtraction of binary digits, a basic question may arise regarding the future utility of enzyme-based computations. We certainly do not consider enzyme-driven computation or logic gate operations as an alternative to conventional computers. We believe, however, that the application of biocatalytic processes for logic gate operations might introduce a new biocomputing paradigm. The availability of numerous biocatalytic systems and coupled enzyme assemblies suggests that a rich variety of logic gates of enhanced complexity and computational power may be envisaged. More specifically, one might consider the design of computing enzymes that follow metabolic pathways or analyze in parallel the therapeutic effectiveness of drugs. Such complex bioprocesses cannot be followed by available computing technologies, and hence, our study points to new facets of biocomputing. Furthermore, it should be noted that recent advances in bioelectronics have demonstrated the possibility of electrically wiring enzymes with electrodes.<sup>17</sup> Thus, an alternative to the optical readout of the operations of the enzyme-based logic gates might be the electrical transduction of these operations. This might not only shorten the response times of these systems and enable the resetting of the biocomputing structure, but allow the construction of wired biocomputing devices. Only further investigations will enable to evaluate the possibilities of implanted biocomputing devices to follow and transduce metabolic processes in the organism or readout drug delivery and therapeutic effectiveness through computational operations.

**Acknowledgment.** This research was supported by the MOLDDYNLOGIC EC project.

## References and Notes

- (1) (a) Credi, A.; Balzani, V.; Langford, S. J.; Stoddart, J. F. *J. Am. Chem. Soc.* **1997**, *119*, 2679–2681. (b) Collier, C. P.; Wong, E. W.; Belohradský, M.; Raymo, F. M.; Stoddart, J. F.; Kuekes, P. J.; Williams, R. S.; Heath, J. R. *Science* **1999**, *285*, 391–394. (c) Kompa, K. L.; Levine, R. D. *Proc. Nat. Acad. Sci. USA* **2001**, *98*, 410–414. (d) de Silva, A. P.; Gunaratne, H. Q. N.; McCoy, C. P. *Nature* **1993**, *364*, 42–44. (e) Shipway, A. N.; Willner, I. *Acc. Chem. Res.* **2001**, *34*, 421–432. (f) Ashton, P. R.; Baldoni, V.; Balzani, V.; Credi, A.; Hoffmann, H. D. A.; Martines-Diaz, M.-V.; Raymo, F. M.; Stoddart, J. F.; Venturi, M. *Chem. Eur. J.* **2001**, *7*, 3482–3493.
- (2) (a) de Silva, A. P.; McClenaghan, N. D. *Chem. Eur. J.* **2002**, *8*, 4935–4945. (b) Lee, S. H.; Kim, J. Y.; Kim, S. K.; Lee, J. H.; Kim, J. S. *Tetrahedron* **2004**, *60*, 5171–5176. (c) Callan, J. F.; de Silva, A. P.; McClenaghan, N. D. *Chem. Commun.* **2004**, 2048–2049. (d) Uchiyama, S.; McClean, G. D.; Iwai, K.; de Silva, A. P. *J. Am. Chem. Soc.* **2005**, *127*, 8920–8921. (e) Straight, S. D.; Andréasson, J.; Kodis, G.; Bandyopadhyay, S.; Mitchell, R. H.; Moore, T. A.; Moore, A. L.; Gust, D. *J. Am. Chem. Soc.* **2005**, *127*, 9403–9409. (f) Remacle, F.; Heath, J. R.; Levine, R. D. *Proc. Natl. Acad. Sci. U.S.A.* **2005**, *102*, 5653–5658.
- (3) (a) Remacle, F.; Willner, I.; Levine, R. D. *ChemPhysChem* **2005**, *6*, 1239–1242. (b) Cheng, P.-N.; Chiang, P.-T.; Chiu, S.-H. *Chem. Commun.* **2005**, 1285–1287. (c) Bag, B.; Bharadwaj, P. K. *Chem. Commun.* **2005**, 513–515. (d) Andréasson, J.; Terazono, Y.; Albinsson, B.; Moore, T. A.; Moore, A. L.; Gust, D. *Angew. Chem., Int. Ed.* **2005**, *44*, 1–5. (e) Margulies, D.; Melman, G.; Shanzer, A. *Nat. Mater.* **2005**, *4*, 768–771. (f) Hod, O.; Baer, R.; Rabani, E. *J. Am. Chem. Soc.* **2005**, *127*, 1648–1649.
- (4) (a) de Silva, A. P.; McClenaghan, N. D. *J. Am. Chem. Soc.* **2000**, *122*, 3965–3966. (b) Brown, G. J.; de Silva, A. P.; Pagliari, S. *Chem. Commun.* **2002**, 2461–2463. (c) Langford, S. J.; Yann, T. *J. Am. Chem. Soc.* **2003**, *125*, 11198–11199. (d) de Silva, A. P.; McClenaghan, N. D. *Chem. Eur. J.* **2004**, *10*, 574–586. (e) Margulies, D.; Melman, G.; Felder, C. E.; Arad-Yellin, R.; Shanzer, A. *J. Am. Chem. Soc.* **2004**, *126*, 15400–15401. (f) Andréasson, J.; Kodis, G.; Terazono, Y.; Lidell, P. A.; Bandyopadhyay, S.; Mitchell, R. H.; Moore, T. A.; Moore, A. L.; Gust, D. *J. Am. Chem. Soc.* **2004**, *126*, 15926–15927.
- (5) de Silva, A. P.; Gunaratne, H. Q. N.; McCoy, C. P. *J. Am. Chem. Soc.* **1997**, *119*, 7891–7892.
- (6) McSkimming, G.; Tucker, J. H. R.; Bouas-Laurent, H.; Desvergne, J.-P. *Angew. Chem., Int. Ed.* **2000**, *39*, 2167–2169.
- (7) Doron, A.; Katz, E.; Portnoy, M.; Willner, I. *Angew. Chem., Int. Ed.* **1996**, *35*, 1535–1537.
- (8) (a) Willner, I. *Acc. Chem. Res.* **1997**, *30*, 347–356. (b) Stojanovic, M. N.; Mitchell, T. E.; Stefanovic, D. *J. Am. Chem. Soc.* **2002**, *124*, 3555–3561. (c) Saghatelian, A.; Völcker, N. H.; Guckian, K. M.; Lin, V. S.-Y.; Ghadiri, M. R. *J. Am. Chem. Soc.* **2003**, *125*, 346–347. (d) Stojanovic, M. N.; Stefanovic, D. *J. Am. Chem. Soc.* **2003**, *125*, 6673–6676. (e) Ashkenasy, G.; Ghadiri, M. R. *J. Am. Chem. Soc.* **2004**, *126*, 11140–11141. (f) Weizmann, Y.; Elnathan, R.; Lioubashevski, O.; Willner, I. *J. Am. Chem. Soc.* **2005**, *127*, 12666–12672.
- (9) (a) Gardner, T. S.; Cantor, C. R.; Collins, J. J. *Nature* **2000**, *403*, 339–342. (b) Elowitz, M. B.; Leibler, S. *Nature* **2000**, *403*, 335–338. (c) Benenson, Y.; Paz-Elizur, T.; Adar, R.; Keinan, E.; Livneh, Z.; Shapiro, E. *Nature* **2001**, *414*, 430–434. (d) Hayes, B. *Am. Sci.* **2001**, *89*, 204–208. (e) Benenson, Y.; Gil, B.; Ben-Dor, U.; Adar, R.; Shapiro, E. *Nature* **2004**, *429*, 423–429. (f) Deonaraine, A. S.; Clark, S. M.; Konermann, L. *FGCS* **2003**, *19*, 87–97.
- (10) Sugita, M. *J. Theor. Biol.* **1961**, *1*, 415–430.
- (11) Arkin, A.; Ross, J. *Biophys. J.* **1994**, *67*, 560–578.
- (12) Zauner, K.-P.; Conrad, M. *Biotechnol. Prog.* **2001**, *17*, 553–559.
- (13) (a) Sivan, S.; Tuchman, S.; Lotan, N. *Biosystems* **2003**, *70*, 21–33. (b) Sivan, S.; Lotan, N. *Biotechnol. Prog.* **1999**, *15*, 964–970.
- (14) Rakitzis, E. T.; Papandreou, P. *Chem.-Biol. Interact.* **1998**, *113*, 205–216.
- (15) Susumu, O.; Makoto, A.; Daisuke, T. *Agric. Biol. Chem.* **1986**, *50*, 2503–2507.
- (16) Kohavi, Z. *Switching and Finite Automata Theory*; Tata McGraw-Hill: New Delhi, 1999.
- (17) (a) Willner, I.; Katz, E. *Angew. Chem., Int. Ed.* **2000**, *39*, 1180–1218. (b) Xiao, Y.; Patolsky, F.; Katz, E.; Hainfeld, J. H.; Willner, I. *Science* **2003**, *299*, 1877–1881. (c) Zayats, M.; Katz, E.; Baron, R.; Willner, I. *J. Am. Chem. Soc.* **2005**, *127*, 12401–12406.